J|A|C|S
ARTICLES
Published on Web 05/15/2002

Resonance Raman Evidence for Protein-Induced Out-of-Plane Distortion of the Heme Prosthetic Group of Mammalian Lactoperoxidase

Steven D. Zbylut and James R. Kincaid*

Contribution from the Chemistry Department, Marquette University, Milwaukee, Wisconsin 53233

Received November 21, 2001. Revised Manuscript Received March 18, 2002

Abstract: Resonance Raman spectra have been acquired for resting state mammalian lactoperoxidase, LPO(N), and its six-coordinate, low-spin (6CLS) cyanide complex, LPO(CN), as well as for various heme l containing fragments resulting from partial or complete proteolytic digestion. These proteolytic fragments provide a useful set of reference compounds for analysis of the LPO(N) and LPO(CN) enzymes, using various ligands to generate well-defined five-coordinate and six-coordinate high-spin (5CHS and 6CHS) species. In addition, these model compounds, which contain zero, one, or two covalently attached ester linkages to polypeptide chains, are quite useful for determining the extent to which the presence of the ester linkages at the heme periphery affects the characteristic heme resonance Raman marker bands. The spectral results not only provide strong evidence for the formulation of the resting state enzyme as a 6CHS species, but also confirm the previously documented anomalous intensities of several low-frequency resonance Raman bands, which are most reasonably interpreted to arise from a protein-induced out-of-plane distortion of the heme l macrocycle mediated by the covalent ester linkages to the associated polypeptide residues of the intact protein.

Introduction

Peroxidases are a class of heme-containing enzymes that utilize and eliminate hydrogen peroxide by catalyzing the oxidation of various inorganic and organic substrates, in the process giving rise to several short-lived enzymatic intermediates which possess ferryl heme moieties and heme- or protein-centered radicals,[1−3] Figure 1. Plant and bacterial peroxidases possess the common protoheme prosthetic group linked to the protein through coordination to a proximal histidine whose basicity is enhanced, relative to the proximal histidine of oxygen transport proteins, myoglobin and hemoglobin, by a hydrogen-bonding interaction of the imidazole proton to a nearby ionized carboxylate residue, for example, aspartate or glutamate.[1] A common feature of the distal side active site of the plant and bacterial peroxidases is the presence of several basic or charged (e.g., arginine) residues which are effective as acid/base catalysts and stabilize the developing negative charge upon cleavage of the O−OH bond, the synergistic effects of the distal and proximal side environments being referred to as the so-called "push−pull" effect.[4]

While the essential elements of plant peroxidase active site structure depicted in Figure 1, including a more basic proximal histidine and distal histidine and arginine residues to promote hydroperoxide bond cleavage, are maintained in the mammalian peroxidases,[5] to the extent that prosthetic group reactivity is controlled by the nature of the active site structure, differences must exist to account for the different reactivity of mammalian peroxidases relative to the plant and bacterial enzymes.[5] One obvious difference, of course, is the fact that mammalian peroxidases possess a chemically derivatized form of heme b, with the 1 and 5 methyl groups of heme b being replaced with hydroxymethyl groups involved in ester linkages with acid residues (Glu275 and Asp125) of the polypeptide, as has been convincingly documented recently by Rae and Goff[6] through carefully conducted chromatographic separation and NMR spectral analysis of proteolytic fragments of LPO (see Figure 2).

Such linkages may impart altered functional properties to the mammalian peroxidase prosthetic groups by several possible mechanisms. First, it is reasonable to suggest that presence of the ester linkages themselves, though removed from the macrocyclic core π system by a methylene group, may alter the electronic properties of the heme by an inductive effect. In addition, it is possible that these ester linkages serve as anchors to provide an effective mechanism for mediation of protein-induced out-of-plane distortion of the heme macrocycle. Such

* To whom correspondence should be addressed. E-mail: James.Kincaid@marquette.edu.

(1) Pruitt, K.; Tenovuo, J. *The Lactoperoxidase System: Chemistry and Biological Significance*; Marcel Dekker: New York, 1985.
(2) Reiter, B.; Perraudin, J. P. In *Peroxidases in Chemistry and Biology*; Everse, J., Everse, K. E., Grisham, M. B., Eds.; CRC Press: Boca Raton, FL, 1991; Vol. 1, pp 143−180.
(3) Thomas, E. L.; Bozeman, P. M.; Learn, D. B. In *Peroxidases in Chemistry and Biology*; Everse, J., Everse, K. E., Grisham, M. B., Eds.; CRC Press: Boca Raton, FL, 1991; Vol. 1, pp 123−142.
(4) Poulos, T.; Kraut, J. *J. Biol. Chem.* **1980**, *255*, 8199−8205.
(5) Poulos, T. In *The Porphyrin Handbook*; Kadish, K. M., Smith, K. M., Guilard, R., Eds.; Academic Press: San Diego, 2000; Vol. 4, pp 189−218.
(6) Rae, T. D.; Goff, H. M. *J. Biol. Chem.* **1998**, *273*, 27968−27977.

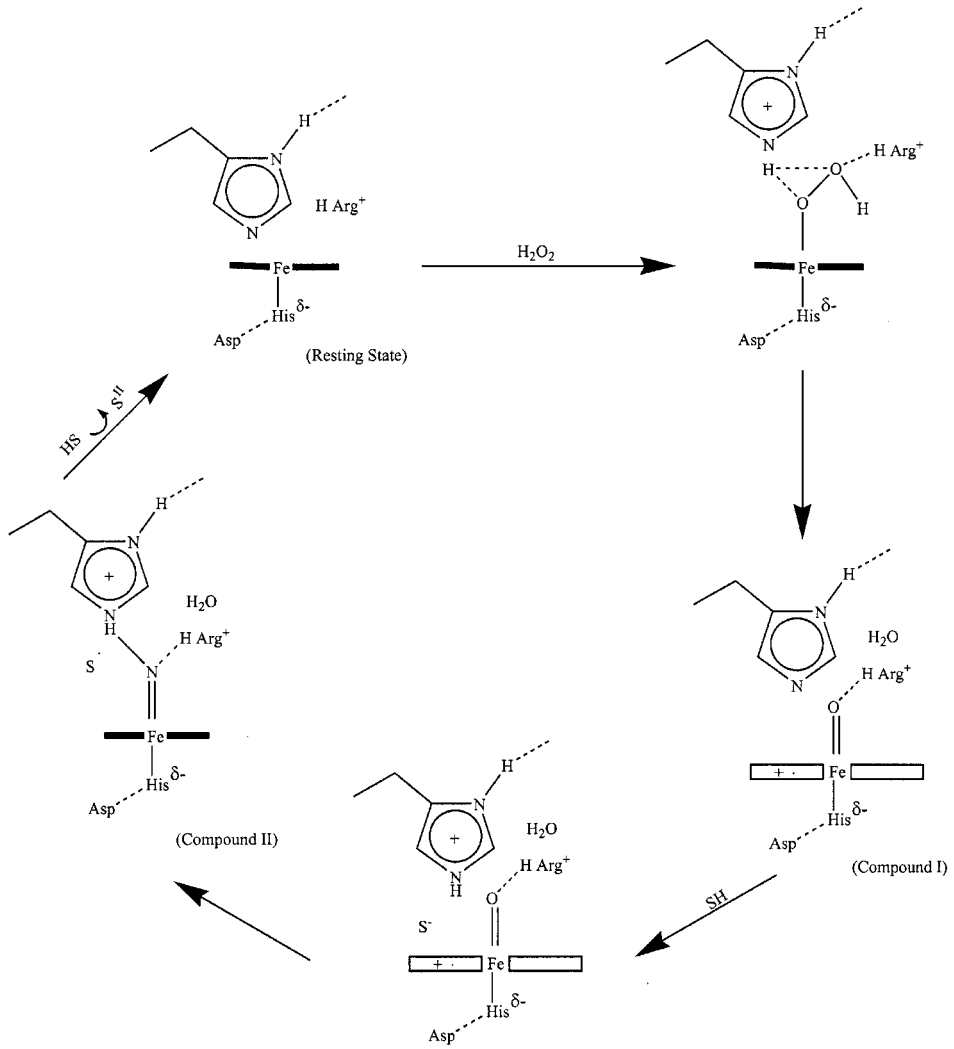

Figure 1. Active site structural features and proposed mechanism for peroxide cleavage.

out-of-plane structures are energetically unfavorable for protein-free metalloporphyrins, but may be induced in certain cases; for example, in synthetically engineered metalloporphyrins bearing bulky substituents, out-of-plane distortions that relieve the steric crowding are well documented.[7−9] While little attention has been paid, until recently,[10−12] to the potential functional consequences of such nonplanar distortions, such possibilities certainly warrant closer investigation. In this regard, it is important to point out that relatively large nonplanar prosthetic group distortions have been documented in the X-ray crystal structure of cytochrome *c*,[13] another heme protein which contains a chemically altered heme b; in this case, the prosthetic group forms covalent thioether linkages between the two peripheral vinyl groups and methionine residues of the polypeptide. Clearly, the ester linkages to the 1- and 5-hydroxymethyl groups of the mammalian peroxidase prosthetic groups may serve a similar function.

To the extent that RR is a powerful probe of heme prosthetic group molecular and electronic structure,[14−18] it may be used to document subtle differences in active site structure of the mammalian peroxidases relative to the plant and bacterial enzymes. An example of particular relevance for the present work is the carefully conducted work by Hu, Spiro, and co-workers[19] on the RR spectra of cytochrome *c*, wherein the appearance of unusually intense features in the low-frequency region was attributed to the activation of out-of-plane modes by a protein-induced distortion mediated by the covalent thioether linkages.

As has been reported previously,[20−24] the RR spectra of the mammalian peroxidase of interest here, LPO, do indeed exhibit

(7) Shelnutt, J. A.; Medforth, C. J.; Berber, M. D.; Barkigia, K. M.; Smith, K. M. *J. Am. Chem. Soc.* **1991**, *113*, 4077−4087.
(8) Medforth, C. J.; Berber, M. D.; Smith, K. M.; Shelnutt, J. A. *Tetrahedron Lett.* **1990**, *31*, 3719−3722.
(9) Brennan, T. D.; Scheidt, W. R.; Shelnutt, J. A. *J. Am. Chem. Soc.* **1988**, *110*, 3919−3924.
(10) Shelnutt, J. A. In *The Porphyrin Handbook*; Kadish, K. M., Smith, K. M., Guilard, R., Eds.; Academic Press: San Diego, 2000; Vol. 7, pp 167−224.
(11) Shelnutt, J. A.; Song, X.-Z.; Ma, J.-G.; Jia, S.-L.; Jentzen, W.; Medforth, C. J. *Chem. Soc. Rev.* **1998**, *27*, 31−41.
(12) Harris, D.; Loew, G. *J. Am. Chem. Soc.* **1993**, *115*, 8775−8779.
(13) Berghuis, A. M.; Brayer, G. D. *J. Mol. Biol.* **1992**, *223*, 959−976.
(14) Spiro, T. G.; Li, X.-Y. In *Biological Applications of Raman Spectroscopy*; Spiro, T., Ed.; Wiley: New York, 1988; Vol. 3, pp 1−37.
(15) Kitagawa, T.; Mizutani, Y. *Coord. Chem. Rev.* **1994**, *135/136*, 685.
(16) Smulevich, G. *Biospectroscopy* **1998**, *4*, S3−S17.
(17) Kincaid, J. R. In *The Porphyrin Handbook*; Kadish, K. M., Smith, K. M., Guilard, R., Eds.; Academic Press: San Diego, 2000; Vol. 7, pp 225−291.
(18) Hu, S.; Smith, K. M.; Spiro, T. G. *J. Am. Chem. Soc.* **1996**, *118*, 12638−12646.
(19) Hu, S.; Morris, I. K.; Singh, J. P.; Smith, K. M.; Spiro, T. G. *J. Am. Chem. Soc.* **1993**, *115*, 12446−12458.
(20) Kimura, S.; Yamazaki, I.; Kitagawa, T. *Biochemistry* **1981**, *20*, 4632−4638.

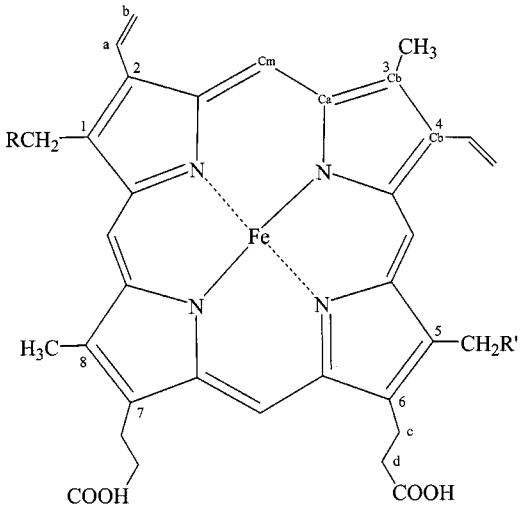

	R	R'
Heme b	H	H
Heme l	OH	OH
Heme l in LPO	$^{275}GluCO_2$	$^{125}AspCO_2$

Figure 2. Peripheral substitution of heme l, heme b, and lactoperoxidase.

unusual features relative to the RR spectra obtained for the plant and bacterial enzymes, most notably a remarkable enhancement of several low-frequency modes, which may be attributable to out-of-plane macrocycle deformation modes.[14−19] The purpose of the present work is to investigate the extent to which such activation of modes is attributable to protein-induced out-of-plane distortions rather than the mere presence of two peripheral ester linkages by acquiring, for the first time, the RR spectra of isolated heme l and its derivatives, including several of the proteolytic fragments originally described by Rae and Goff,[6,25] under well-controlled conditions so as to provide a set of reference spectra appropriate for interpretation of the LPO spectral data.

Experimental Section

Materials. The LPO samples were isolated and purified from cows' milk obtained from a local dairy farmer, using procedures previously reported.[26] The purities of the final preparations were determined by measuring the so-called Rz value (A_{412}/A_{280}), in all cases this value being greater than 0.90. In accordance with procedures previously described by Rae and Goff,[6] individual proteolytically cleaved fragments of LPO were isolated by preparative reverse-phase HPLC, the chromatographic results being depicted in Figure 3. The chromatogram depicted in trace A of Figure 3 represents that obtained using proteolytic enzymes (trypsin and proteinase K), designated PK digestion, and conditions that maximize the amount of free heme l (designated PK2 in the chromatogram), whereas that shown in trace B is derived from a different set of enzymes (trypsin and chymotrypsin), designated TC digestion, and conditions that give rise to larger amounts of species which retain one or two peptide fragments connected to the heme l

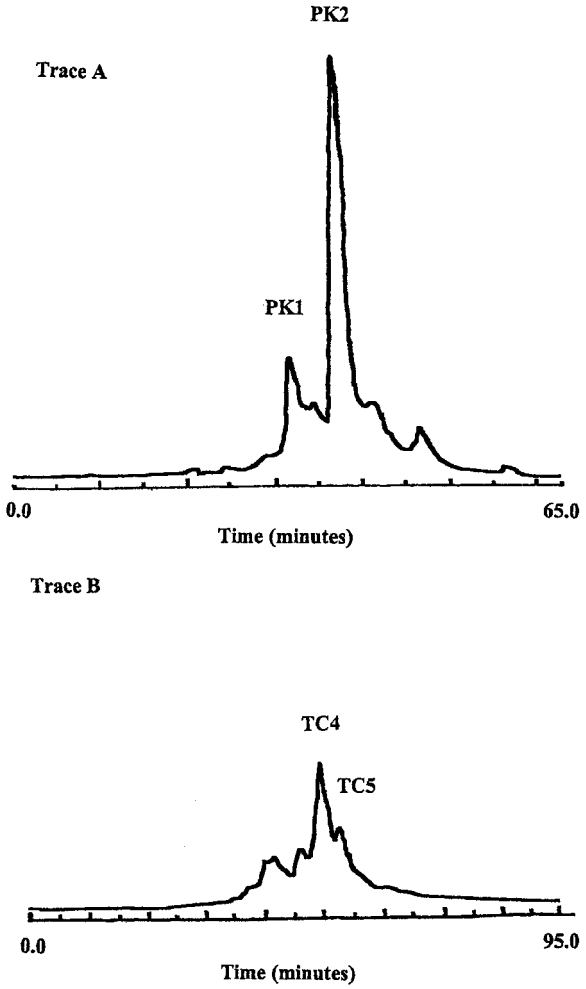

Figure 3. Chromatograms of proteolytic digests. Trace A: Sample from PK digestion prcoedure. Trace B: Sample from TC digestion procedure.

through ester linkages. While the actual retention times of the peaks depicted in the chromatograms of Figure 3 understandably do not precisely match those originally reported,[6] the general chromatographic profiles do coincide with those reported; that is, the number of major components and their relative intensities do correspond rather closely with those reported, although the chromatographic resolution of the chromatograms obtained here is somewhat lower than the high-quality, analytical scale data reported earlier.[6] Thus, in trace A the strongest peak (labeled PK2) is properly associated with free heme l, a fact confirmed by comparison of the high-resolution NMR spectrum (Figure 4) of the isolated fragment to that previously reported by Rae and Goff.[6] Here, and in the original report,[6] the strongest peak appearing at shorter retention times, designated PK1, is associated with a species bearing a single covalently attached peptide fragment at position 1. In a similar fashion, several of the fragments isolated from the second type of proteolytic digestion procedure, whose chromatographic profile is depicted in trace B of Figure 3, were collected and used for the RR studies. Finally, it is important to emphasize that only those fractions that are associated with major, clearly isolated components were used for the spectroscopic studies, that is, only those labeled PK1 and PK2 from the PK digestion and TC5 from the TC digestion. Nevertheless, these three proteolytic fragments provide a complete set of reference compounds for the present purposes in that they represent species with zero, one, or two covalently attached peptide chains.

Methods. The high-performance liquid chromatographic separations were performed on an ISCO HPLC system with a variable wavelength UV detector set at 400 nm. The column used for this separation was a semipreparative reverse-phase C18 column (10 mm × 25 cm) with a

(21) Manthey, J.; Boldt, N.; Bocian, D.; Chan, S. *J. Biol. Chem.* **1986**, *261*, 6734−6741.
(22) Reczek, C.; Sitter, A.; Terner, J. *J. Mol. Struct.* **1989**, *214*, 27−41.
(23) Hu, S.; Treat, R.; Kincaid, J. R. *Biochemistry* **1993**, *32*, 10125−10130.
(24) Hu, S.; Kincaid, J. R. *J. Am. Chem. Soc.* **1991**, *113*, 7189−7194.
(25) Rae, T.; Goff, H. *J. Am. Chem. Soc.* **1996**, *118*, 2103−2104.
(26) Hultquist, D.; Morrison, M. *J. Biol. Chem.* **1963**, *238*, 2847−2849.

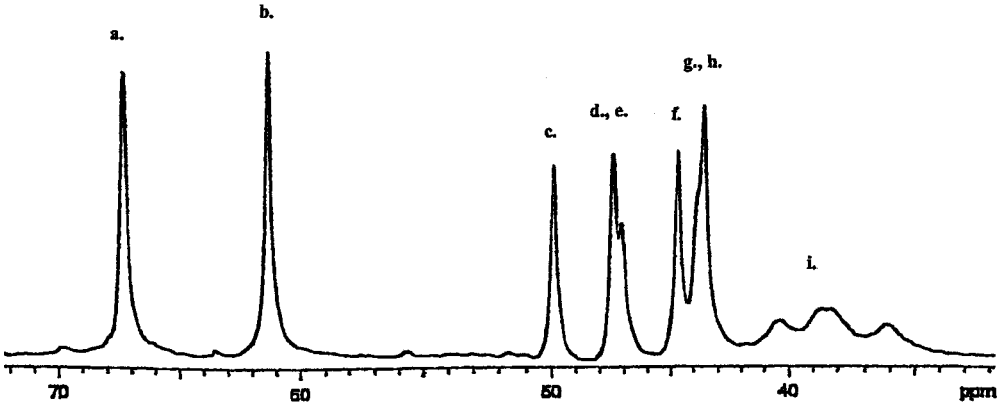

Figure 4. NMR spectrum of the PK2 fragment. The peaks and assignments are as follows: (a) 67.3 ppm, 8-methyl; (b) 61.3 ppm, 3-methyl; (c) 49.9 ppm, α-propionyl-CH_2; (d) 47.4 ppm, hydroxymethyl; (e) 47.1 ppm, α-vinyl-CH; (f) 44.7 ppm, α-propionyl-CH_2; (g) 43.9 ppm, hydroxymethyl; (h) 43.6 ppm, α-vinyl-CH; (i) 40.3, 38.7, 38.3, and 36.2 ppm, methine CH.

particle size of 10 μm (Alltech, 28085). The separation required the use of a static loading phase (0−5.0 min) to load the sample onto the column, followed by a linear gradient to elute the proteolytic fragments (5.0−65.0 min for the PK digest and 5.0−95.0 min for the TC digest). The elution was conducted at a flow rate of 3.0 mL/min.

All fractions that eluted from the column with an absorbance reading greater than 0.1 absorbance units at 400 nm were collected. Using a 1 cm quartz cuvette and a HP8452A diode array spectrophotometer, these multiple fractions were then analyzed prior to pooling, the most strongly absorbing fractions from a given peak being pooled.

The paramagnetic ^{1}H NMR spectrum of the PK2 sample was recorded on a Bruker AMX-600 FT NMR spectrometer. Chemical shift values are referenced to the residual DMSO signal at 2.5 ppm, calibrated in turn with TMS. The ^{1}H NMR spectrum was obtained by dissolving the heme l (PK2) in DMSO-d_6 (Aldrich Chemical). The ^{1}H NMR spectrum for the high-spin bis(DMSO) Fe(III) heme complex (30−50 μM) was obtained over a 120 kHz spectral width and was acquired with a repetition rate of 20 s^{-1}.

The LPO(N) and LPO(CN) compounds were prepared in an aqueous buffer system (100 mM sodium phosphate buffer (pH = 7.4)). The LPO(N) was used as obtained after extraction from bovine milk, while the LPO(CN) compound was prepared by adding a small amount of KCN (Aldrich) to the LPO(N) species. The conversion of LPO(N) to the LPO(CN) was judged complete by examination of the UV−vis absorption spectra.[27]

The low-spin six-coordinate model compounds (PK1, PK2 (heme l), and TC5) were prepared in an aqueous buffer system (100 mM sodium phosphate buffer, pH = 7.4, containing 70 mM *N*-methylimidazole). The *N*-methylimidazole (*N*-MIm) was purified prior to use by vacuum distillation.

The high-spin five-coordinate model compounds (PK1 and PK2 (heme l)) were prepared in an aqueous buffer system (100 mM sodium phosphate buffer, pH = 7.4, containing 70 mM 2-methylimidazole). The 2-methylimidazole (2-MIm) solution was purified by sublimation.

The high-spin six-coordinate model compounds (PK1 and PK2 (heme l)) were dissolved in DMSO-d_6 (Aldrich Chemical). No further steps were needed to prepare these species.

All resonance Raman (RR) measurements were taken with either a Spex 1269 single monochromator that was connected to a charge-couple device (CCD) (Princeton Instruments, Model ICCD-576LD/GRB) or a Spex 1403 double monochromator that was connected to a photomultiplier tube (PMT). The samples were illuminated with a Coherent Innova 100-K3 Krypton ion laser using various laser lines, including the 406.7 and 413.1 nm lines. The CCD was controlled by a Northgate computer equipped with the CCD Spectrometric Multichannel Analysis Software (Version 2.1) program, while the PMT was interfaced with a Spex Model DM1B computer. Samples contained in a 5 mm i.d. NMR tube were positioned in a 135° scattering geometry and were kept spinning during laser illumination. All resonance Raman spectra have been background corrected. All spectra recorded are accurate to within ±2 cm^{-1}.

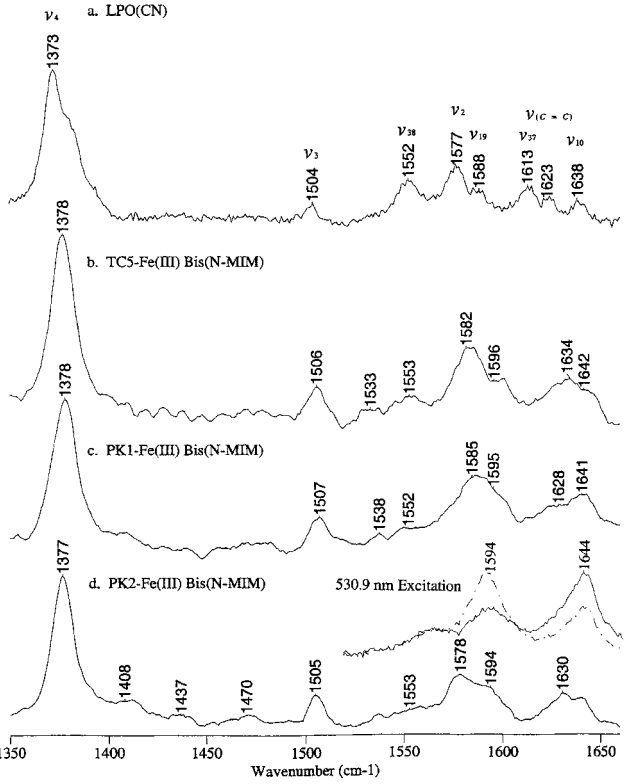

Figure 5. Resonance Raman spectra of LPO(CN) and 6CLS species. High-frequency resonance Raman spectroscopy of (a) LPO(CN), (b) TC5-Fe(III) bis(*N*-MIm), (c) PK1-Fe(III) bis(*N*-MIm), and (d) PK2-Fe(III) bis(*N*-MIm). All samples were dissolved in 0.10 M phosphate buffer (pH 6.8) and excited with 413.1 nm, 20 mW power at the sample. Each spectrum is an average of 16 scans (scan speed is 2 cm^{-1} s^{-1}). Spectra were acquired with the Spex 1403 spectrometer, while the spectra shown in the inset were acquired with the Spex 1269/ccd spectrometer using 530.9 nm excitation (parallel polarization, solid line; perpendicular polarization, dashed line).

Results

High-Frequency Region. Figures 5−7 show the RR spectra acquired for ferric LPO and selected proteolytic fragments in

(27) Andersson, L.; Bylkas, S.; Wilson, A. *J. Biol. Chem.* **1996**, *271*, 3406−3412.

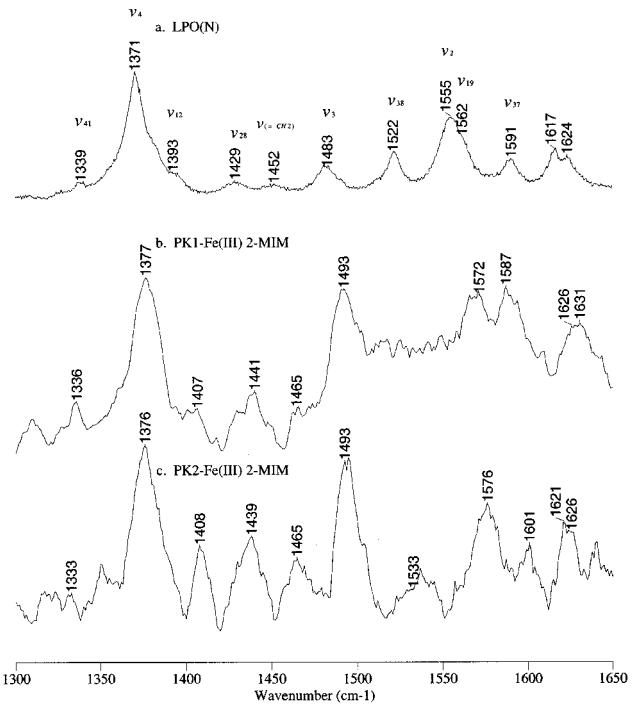

Figure 6. High-frequency resonance Raman spectra of LPO(N) and 5CHS models. High-frequency resonance Raman spectroscopy of (a) LPO(N), (b) PK1-Fe(III) 2-MIm, and (c) PK2-Fe(III) 2-MIm. All samples were dissolved in 0.10 M phosphate buffer (pH 6.8) and excited with 406.7 nm, 20 mW power at the sample. Spectra were acquired with the Spex 1403 spectrometer; each spectrum is an average of 16 scans (scan speed is 2 cm^{-1} s^{-1}).

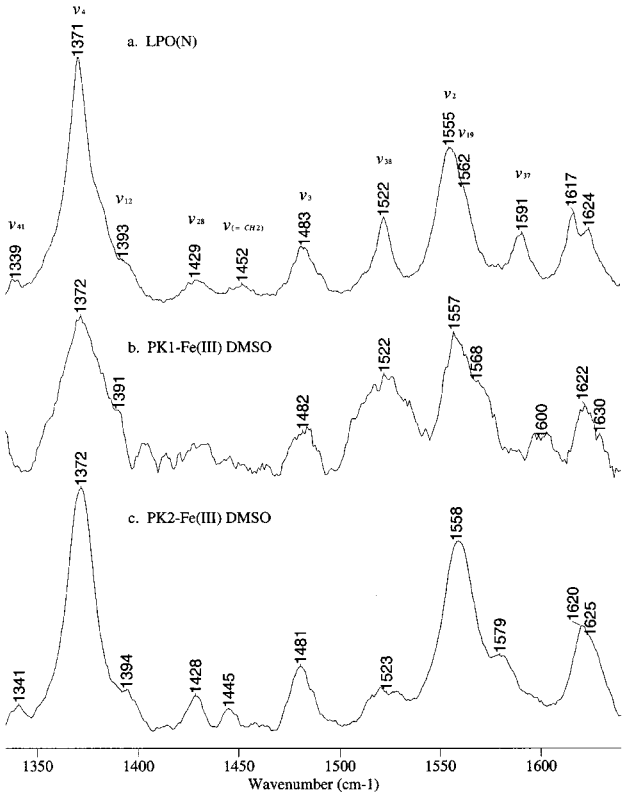

Figure 7. High-frequency resonance Raman spectra of LPO(N) and 6CHS models. High-frequency resonance Raman spectroscopy of (a) LPO(N), (b) PK1-Fe(III) DMSO, and (c) PK2-Fe(III) DMSO. The LPO(N) sample was dissolved in 0.10 M phosphate buffer (pH 6.8), while the model compounds were prepared in DMSO-d_6. The RR spectra were acquired with the 406.7 nm laser line, 20 mW power at the sample. Spectra were acquired with the Spex 1403 spectrometer; each spectrum is an average of 16 scans (scan speed is 2 cm^{-1} s^{-1}).

various spin- and coordination states, with the frequencies and the most reasonable assignments, based on comparison with the results of many other heme protein RR spectral studies,[14−22] being listed in Table 1. Addition of excess *N*-methylimidazole (*N*-MIm) to model heme complexes results in the formation of six-coordinate, low-spin species (6CLS), the spectra of three such models being shown in the bottom three traces of Figure 5, with the spectrum of the 6CLS cyanide complex of LPO, LPO(CN), being given in the top trace for comparison. While there are slight differences in the spectral pattern observed for LPO(CN) in comparison with those observed for the models (vide infra), it is important to note the strong similarity in the latter set of spectra. Thus, even though the complexes derived from the different proteolytic fragments (PK1, PK2, and TC5) possess different numbers of covalently linked peptides (i.e., one, zero, and two, respectively), these ester linkages exert little effect on the observed high-frequency RR spectral patterns; that is, the presence of the ester linkages, in themselves, does not significantly alter the RR spectral pattern.

In Figures 6 and 7 are illustrated the RR spectra of the 5CHS and 6CHS model compounds, respectively, along with the spectrum acquired for native, resting state LPO, LPO(N). The assignments for the observed bands, indicated directly in the figures and in Table 1, are consistent with the results obtained for other heme proteins[14−19] and those previously given for LPO(N).[21,22] In comparing the spectra illustrated in these two figures, the most obvious point to emerge is that, in general, the spectral patterns observed for the 6CHS bis-DMSO model compounds (Figure 7) are much more similar to that obtained for the native enzyme (top trace of each figure) than are the patterns observed for the 5CHS 2-MIm models (Figure 6). Thus, not only the frequencies, but also the approximate relative intensities, of the modes observed in the bottom two traces displayed in Figure 7 are quite closely matched with those shown in the top trace, that is, those for LPO(N).

In contrast to the similarity of spectral patterns shown in Figure 7, several distinct and important differences in the spectra obtained for the 5CHS models with that obtained for the native LPO are apparent (Figure 6). Thus, in both of the model spectra, the strong ν_4 mode is observed at 5−6 cm^{-1} higher frequency than for LPO(N). Most significantly, the reliable spin- and coordination state marker band, ν_3, is observed near 1493 cm^{-1} for the two models, a value that is entirely consistent with that expected for a 5CHS heme,[14−18] whereas it is observed 10 cm^{-1} lower for LPO(N) at 1483 cm^{-1}. While the other reliable spin-state marker, ν_{10}, can be seen as a weak feature near 1644 cm^{-1} in the spectra of the 6CLS species shown in Figure 5, as is often the case for HS complexes, this mode (expected nearer 1610 cm^{-1}) overlaps modes associated with the vinyl substituents and is not as easily identified. Finally, significantly different patterns are observed in the 1550−1570 cm^{-1} region in Figure 6, a region wherein the ν_2 mode is expected. In the spectra of the models the ν_2 modes are observed above 1570 cm^{-1}, values that are consistent with a 5CHS configuration,[14−18] and approximately 15−20 cm^{-1} higher than that of the LPO(N). This also is in stark contrast to the set of spectra shown in Figure 7 for the 6CHS models, where the approximate intensities and frequencies for the ν_2 modes of the models match very well with those observed for the enzyme. Thus, comparison of the

Table 1. [a]

modes	MetMb	LPO(N)	FePK2(DMSO)$_2^+$	FePK2(2MIm)$^+$	FePK2(NMIm)$_2^+$	LPO(CN)
ν(C═C)	1621s				1630w	1623m
		1624/1617m[b]	1625/1620m[b]	1626/1621m[b]		
ν_{10}	1608vw				1644	1638w
ν_{37}	1583w	1591m	1579w	1601w		1613m
ν_{19}		1562w			1594w	1588m
ν_2	**1563vs**	**1555s**	**1558s**	**1576m**	**1578m**	**1577m**
ν_{11}	1544w					
ν_{38}	1511w	1522m	1523w	1533w,br	1553vw	1552s
ν_3	**1483m**	**1483m**	**1481m**	**1493s**	**1505m**	**1504s**
δ(═CH$_2$)	1451w	1452vw	1445vw	1465w	1470vw	
ν_{28}	1426m	1429w	1428w	1439m	1437vw,br	
ν_{29}	1402vw			1408m	1408vw	
ν_{12}	1389w	1393w	1394w			
ν_4	**1373vs**	**1371vs**	**1372vs**	**1376s**	**1377vs**	**1373vs**
ν_{41}	1341w	1339vw	1341vw	1333vw		1345w
δ(C$_a$H═)	1316/1301vw	1310/1302vw	1315	1319/1295	1313	1307
CH$_2$ wag	1282vw	1284w		1270	1281	1288
CH$_2$ twist	1223w	1229vw		1240	1224	1239
ν_{13}	1209w	1215w	1214	1210	1210	
ν_{30}	1169m	1173w		1184	1173	1174
ν_{14}	1135m	1136		1145	1131	1135
ν_5	1121m	1124m	1126	1127	1115	1117
δ(═CH$_2$)	1092/1048vw	1094	1054	1093/1052	1091/1036	1080
ν_{45}(C−V)	1007w	996m	1008	1004	1004	991
γ(CH═)	989w	982w		969	993	
ν_{46}	930w	934vw	929	933	949	941
γ(═CH$_2$)	919w	925vw	914		924	915
ν_{15}	757vw	756m	760	754	745	746w
γ_5	721w	718vw		727	737	
γ_{11}	715w	709w	713w	711w	709	710w
ν_7	674s	678s	679s	679s	681s	677s
ν_{48}	584vw	575/569vw	566w	569vw,br	560w	
γ_{21}	547w	548vw	550vw			
		527vw	533vw			
γ_{12}	502w	500/493w	492vw	500w,br	495w,br	508w
ν_{33}	475vw	483w	481vw	482w,br		481vw
		461w			454w,br	459vw
δ(C$_B$C$_a$C$_b$)	440w/409w	433w/**413vs**[c]	439vw/**411w**	425vw,br	425vw/**405vw**	432w/**415s**[c]
δ(C$_B$prop)	378s			374w		
γ_6	**337w**	**335s**[d]	**338vw**		356w	**335ms**[d]
ν_8	344m	335s[d]	352m	349m/s	342m	335ms[d]
γ_7	305m	292w	303w	286m,br	319w	310m
ν_9/ν_{52}	248/271	262w,br	263w,br	286,m,br	275w	256/275w

[a] Mode characteristics: s, strong; m, medium; w, weak; br, broad. [b]Vinyl modes and ν_{10} overlap. [c]δ(C$_B$C$_a$C$_b$) or strongly enhanced out-of-plane mode. [d]ν_8 or γ_6, labeling needed.

high-frequency RR spectra shown in Figures 6 and 7 strongly suggests that the resting state LPO(N) enzyme is properly considered as a 6CHS species.

Low-Frequency Region. Given the fact that the high-frequency spectra of the 6CHS models most closely resemble that obtained for the resting state enzyme, attention is focused on the low-frequency spectra of the 6CHS models, that is, Fe(PK1)(DMSO)$_2^+$ and Fe(PK2)(DMSO)$_2^+$.

The low-frequency RR spectra of LPO(N) and the 6CHS PK1 and PK2 models are shown in Figure 8, the frequencies and assignments, along with those of the 6CLS and 5CHS species (spectra not shown), being listed in Table 1. The most obvious difference observed between the spectrum of the LPO(N) and those of the two model compounds is the remarkably strong enhancement of two modes located at 413 and 335 cm^{-1} in the spectrum of the enzyme (top trace), this striking intensity enhancement of these two modes for resting state LPO having been noted previously.[20,21] These differences between the spectrum of the protein and those of the models are also observed for the low-spin species shown in Figure 9, where the 415 and 335 cm^{-1} features in the spectrum of LPO(CN) are again quite strong. In the spectrum of the enzyme it is noted that two other reasonably strong features are observed at 359 and 310 cm^{-1}. As has been shown elsewhere,[23] the 359 cm^{-1} band is assignable to the ν(Fe−CN) stretching mode on the basis of shifts observed upon isotopic substitution of the axial cyanide ligand. Furthermore, it was noted in that work that the 310 cm^{-1} mode is also slightly sensitive to such isotopic substitution, behavior commonly attributed to coupling of ν(Fe−XY) or δ(Fe−XY) axial ligand modes to out-of-plane heme macrocycle modes; for example, a mode near 300 cm^{-1} in the RR spectrum of compound III of LPO also exhibits a small (3 cm^{-1}) shift upon replacing $^{16}O_2$ with $^{18}O_2$.[24]

In contrast to the spectral pattern observed for the enzyme, those observed for the models are quite similar to those observed for other protoheme model compounds and prosthetic groups of most heme proteins,[14−18] where the low-frequency region (below 700 cm^{-1}) is dominated by a relatively intense ν_7 heme core mode occurring near 675 cm^{-1}, with all other modes being of much lower intensity. Again, it is noted that in both Figure 8 and Figure 9 quite similar spectral patterns are observed for the model compounds of a given type, the presence of the ester functionalities, in themselves, not substantially affecting the frequencies or relative intensities.

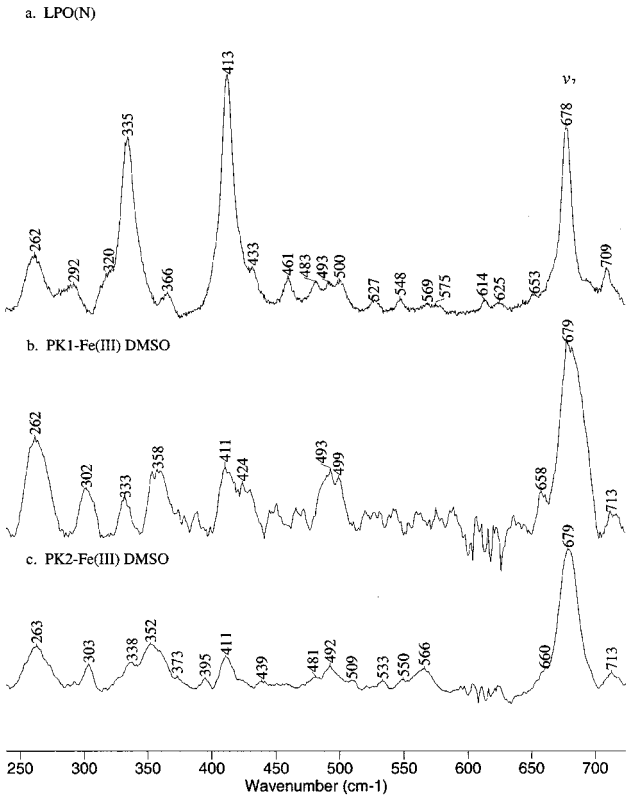

Figure 8. Low-frequency resonance Raman spectra of LPO(N) and 6CHS models. Low-frequency resonance Raman spectroscopy of (a) LPO(N), (b) PK1-Fe(III) DMSO, and (c) PK2-Fe(III) DMSO. The LPO(N) sample was dissolved in phosphate buffer (pH 6.8), while the model compounds were prepared in DMSO-d_6; the Raman spectrum of DMSO-d_6 was subtracted from the spectra of the models to cancel strong solvent bands from the spectra. The RR spectra were acquired with the Spex 1403 spectrometer using 406.7 nm, 20 mW power at sample. Each spectrum is an average of 16 scans (scan speed is 2 cm^{-1} s^{-1}).

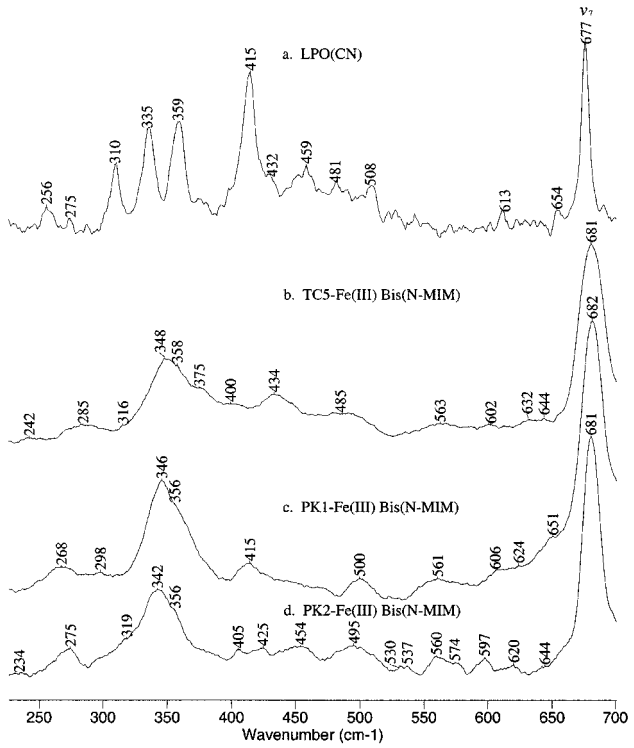

Figure 9. Low-frequency resonance Raman spectra of LPO(CN) and 6CLS models. Low-frequency resonance Raman spectroscopy of (a) LPO(CN), (b) TC5-Fe(III) bis(*N*-MIm), (c) PK1-Fe(III) bis(*N*-MIm), and (d) PK2-Fe(III) bis(*N*-MIm). All samples were dissolved in 0.10 M phosphate buffer (pH 6.8) and excited with 413.1 nm, 20 mW power at the sample. Spectra were acquired with the Spex 1403 spectrometer; each spectrum is an average of 16 scans (scan speed is 2 cm^{-1} s^{-1}).

While the availability of definitive isotopic shift data for selectively labeled LPO analogues, which may eventually become available,[28] would obviously help solidify assignments of low-frequency modes, in their absence it is reasonable to rely on comparisons with low-frequency data obtained for other heme proteins, such as met-myoglobin,[18] keeping in mind the possible effects of heme macrocycle distortion as is seen for cytochrome *c*,[19] vide infra. The suggested assignments, based on these considerations, are given in Table 1 and referred to further in the next section.

Discussion

One previously unresolved issue regarding resting state LPO is the determination of the nature and disposition of axial ligands. While results of various spectroscopic studies are all consistent with a ferric high-spin formulation, uncertainty persists with regard to whether it is 5CHS[29,30] or 6CHS.[20−22,27,31,32] The present results, documenting a much closer similarity of the high-frequency spectral pattern of LPO(N) to those of the 6CHS bis-DMSO complexes, rather than the 5CHS models, provide further support for the 6CHS formulation.

While the resting state enzyme, LPO(N), and 6CHS models exhibit rather similar spectral patterns in the high-frequency region, in the lower-frequency region the spectra of the models deviate substantially from that of the protein (Figures 8), the most notable difference being the remarkably strong intensities of several modes in the latter, especially those observed near 413 and 335 cm^{-1}. A similar intensity enhancement of several modes is observed on comparing the low-frequency spectra of the LPO(CN) derivative with those of the 6CLS models (Figure 9), with the reminder that the presence of the CN^- axial ligand gives rise to the 359 cm^{-1} ν(Fe−CN) mode which also couples with the 310 cm^{-1} oop heme mode.[23,24]

It seems unreasonable to ascribe the anomalous intensity enhancement of these low-frequency modes to differences in axial ligation (proximal histidyl-imidazole vs DMSO or bis-NMIm vs imidazole/CN^-) inasmuch as no such remarkably intense features are seen for other protoheme models or other protoheme-containing heme proteins, for example, myoglobin, hemoglobin, cytochrome P450, or even plant and bacterial peroxidases.[14−19] In fact, to our knowledge, the only heme protein, other than the mammalian peroxidases, which has been shown to exhibit such unusually strong enhancement of modes in the low-frequency RR spectra is cytochrome *c*. Thus, Hu, Spiro, and co-workers,[19] exploiting the possibility of preparing several useful selectively deuterated analogues of the native protein, provided a comprehensive and thoughtful analysis of a large body of carefully acquired RR spectral data for ferric and

(28) Kincaid, J. R.; Colas, K.; Czarnecki, K.; Ortiz de Montellano, P., work in progress.
(29) Shiro, Y.; Morishima, I. *Biochemistry* **1986**, *25*, 5844−5849.
(30) Modi, S.; Behere, V.; Mitra, S. *J. Inorg. Biochem.* **1990**, *38*, 17−25.
(31) Goff, H.; Gonzalez-Vergara, E.; Ales, D. *Biochem. Biophys. Res. Commun.* **1985**, *133*, 794−799.
(32) Chang, C.; Sinclair, R.; Khalid, S.; Yamazaki, I.; Nakamura, S.; Powers, L. *Biochemistry* **1993**, *32*, 2780−2786.

ferrous cytochrome *c*, concluding that one of the most dramatic peculiarities of the observed spectra is strikingly large intensities of several low-frequency out-of-plane modes.

The authors of the above referenced work make convincing arguments to support the contention that the enhancement of low-frequency out-of-plane modes, as well as the appearance of relatively strongly enhanced nontotally symmetric RR modes and nominally IR-active E_u modes, under Soret excitation, are the spectral consequences of protein-induced out-of-plane distortions of the heme macrocyle, a distortion clearly documented in the X-ray crystal structure of that protein,[13] the distortion being mediated through covalent linkages involving the heme vinyl substituents and methionine residues of the polypeptide. As in the case of cytochrome *c*, where one of the strongest low-frequency out-of-plane modes essentially disappears when the protein is unfolded by denaturation,[19] the intensities of the 413 and 335 cm^{-1} bands in the spectrum of LPO(N) and LPO(CN) have no strong counterparts in the spectra of the proteolytic fragments of LPO studied here, even in those cases where the fragments possess ester linkages to associated peptide chains; that is, as in the case of cytochrome *c*, these spectral consequences for LPO(N) are most reasonably attributed to protein-induced out-of-plane distortions of the macrocycle mediated by covalent ester linkages with the acid residues of the polypeptide, the distortion being effectively relaxed upon cleavage of the prosthetic group from the protein.

Some comment is warranted regarding the positions of the high-frequency structure-sensitive core modes in comparing the spectra of the LPO(N) and LPO(CN) with their corresponding models. Thus, in one of the first detailed studies of the effects of nonplanar distortions, Czernuszewicz et al.[33] compared the RR spectra obtained for nickel octaethylporphyrin, NiOEP, in solution with those obtained for triclinic and tetragonal crystalline forms, which contain, respectively, nearly planar and severely ruffled forms of the NiOEP.[34,35] The essential points to emerge from these works are that, in addition to the activation and enhancement of several low-frequency out-of-plane modes, nonplanar distortion of the NiOEP macrocycle leads to a general lowering of high-frequency core modes, especially those associated with the $\nu_{asym}(C_\alpha-C_m)$ methine bridge modes (ν_{10} and ν_{19}); that is, in comparison with the spectra of the triclinic crystals, the ν_{10} and ν_{19} modes shift down by about 20 cm^{-1} for the tetragonal form, while others, such as ν_2 and ν_3, shift down by about 10 cm^{-1}. The observation of ν_{10} and ν_{19} modes in solutions of NiOEP exhibiting frequencies about 10 cm^{-1} lower than those observed for the planar triclinic crystals is generally accepted as confirmation of the presence of a highly ruffled form of NiOEP in solution.[10,11,33−35]

Given the fact that, among the high-frequency core modes, ν_{10} and ν_{19} apparently exhibit the greatest sensitivity to nonplanar distortions, and that these nontotally symmetric modes are most effectively enhanced with Q-band excitation, RR spectral data (shown in the inset in Figure 5) were collected for the 6cls model using 531 nm excitation, to more precisely locate the positions of these modes; the corresponding values for the LPO(CN) were reported in an earlier work.[21] For the 6chs models, the spectral quality with green excitation was very poor, preventing determination of these frequencies; careful measurements of the feature located at 1579 cm^{-1} using Soret excitation show it is a polarized mode, most reasonably assigned as ν_{37}. As can be determined from inspection of the data given in Table 1, both ν_{10} and ν_{19} shift to lower frequencies by about 6 cm^{-1} in comparing the values for LPO(CN) with that of the corresponding 6cls model.

While such behavior is indeed consistent with the proposed nonplanar distortion in the enzyme relative to the protein-free models, some caution is required in drawing such comparisons. Thus, although the results of systematic studies of well-defined systems, such as those conducted for NiOEP referred to above, indicate that nonplanar distortions can affect the positions of these high-frequency core modes, their sensitivity to other structural variations, especially changes in axial ligation, may compromise their utility as indicators of nonplanar distortions. This point has been emphasized in several recent works dealing with other structurally well-defined systems.[36−39] For example, Shelnutt and co-workers, in their studies of nickel-substituted cytochrome *c*[36] and a corresponding nickel-substituted microperoxidase,[37] as well as Othman et al.[38] in their study of a different microperoxidase, point out the ambiguity caused by axial ligation changes in interpreting such spectroscopic data and were careful to interpret changes in core mode frequencies as being reflective of nonplanar distortions only for those species known to share a common coordination environment. Similarly, in a recent comprehensive and thoughtful analysis of the RR spectra of petroporphyrins, Czernuszewicz et al.[39] point out that, while detailed analysis of the ν_{10} and ν_{19} frequencies of NiOEP in solution has led to some controversies regarding the number of coexisting conformers, the activation of oop modes below 850 cm^{-1} leaves no doubt that the solution structure deviates strongly from planarity (p 318 of ref 39). Furthermore, comparisons of data for many more examples presented in that work lead to the conclusion that such activation of low-frequency modes, sometimes including ν_8 and ν_9, is probably a more reliable indicator of nonplanar distortions.

Acknowledgment. This work was supported by a grant from the National Institutes of Health (DK35153) and funds provided for the Pfletschinger Habermann Chair of Chemistry (J.R.K.). The authors express their sincere thanks to Dr. Tracy Rae and Professor Harold Goff for valuable guidance in performing the chromatographic separations and the acquisition of the 600 MHz NMR spectrum of the PK2 sample. The authors also thank Professor Dale Noel of Marquette University's Department of Biology for use of the preparative HPLC equipment, as well as Dr. Kazimierz Czarnecki and Mr. Guangzhi Yuan of the Chemistry Department of Marquette University for acquisition of certain spectra.

JA012578U

(33) Czernuszewicz, R. S.; Li, X.-Y.; Spiro, T. G. *J. Am. Chem. Soc.* **1989**, *111*, 7024−7031.
(34) Li, X.-Y.; Czernuszewicz, R. S.; Kincaid, J. R.; Spiro, T. G. *J. Am. Chem. Soc.* **1989**, *111*, 7012−7023.
(35) Alden, R. G.; Crawford, B. A.; Doolen, R.; Ondrias, M. R.; Shelnutt, J. A. *J. Am. Chem. Soc.* **1989**, *111*, 2070−2072.
(36) Ma, J.-G.; Laberge, M.; Song, X.-Z.; Jentzen, W.; Jia, S.-L.; Zhang, J.; Vanderkooi, J. M.; Shelnutt, J. A. *Biochemistry* **1998**, *37*, 5118−5128.
(37) Ma, J.-G.; Vanderkooi, J. M.; Zhang, J.; Jia, S.-L.; Shelnutt, J. A. *Biochemistry* **1999**, *38*, 2787−2795.
(38) Othman, S.; Le Lirzin, A.; Desbois, A. *Biochemistry* **1994**, *33*, 15437−15448.
(39) Czernuszewicz, R. S.; Maes, E. M.; Rankin, J. G. In *The Porphyrin Handbook*; Kadish, K. M., Smith, K. M., Guilard, R., Eds.; Academic Press: San Diego, 2000; Vol. 7, pp 293−338.